Elastic $p_\uparrow p_\uparrow$ scattering between 240 and 470 MeV

Y. Onel,* R. Hausammann,† E. Heer, R. Hess, C. Lechanoine-Leluc,
W. R. Leo,‡ and D. Rapin
Département de Physique Nucléaire et Corpusculaire, Université de Genève, 1211 Geneva 4, Switzerland

S. Jaccard§ and S. Mango
Paul Scherrer Institute, 5234 Villigen, Switzerland
(Received 16 November 1988)

The polarization parameter P_{n000}, the two-spin parameters D_{n0n0}, K_{n00n}, $D_{s'0s0}$, $D_{s'0k0}$ and the three-spin parameters $M_{s'0sn}$ and $M_{s'0kn}$ have been measured for *pp* elastic scattering angles between 60° and 88° center of mass at 241 and 314 MeV incident kinetic energies, and between 38° c.m. and 98° c.m. at 341, 366, and 398 MeV. At 473 MeV, only P_{n000} and $D_{s'0k0}$ were measured between 34° c.m. and 62° c.m. The experiment was performed at SIN using a polarized proton beam and a polarized butanol target. The polarization of the scattered proton was analyzed in a carbon polarimeter. The influence of these high-precision data on the Saclay-Geneva phase-shift analysis is discussed.

I. INTRODUCTION

The goal of the experimental program on $p_\uparrow p_\uparrow$ elastic scattering at the Paul Scherrer Institute (PSI) (formerly SIN) was to measure, between 400 and 579 MeV, enough spin-dependent observables[1–4] to perform a direct reconstruction of the five complex scattering amplitudes.[5–8] The present low-energy data (241–473 MeV) have been measured to complete this program and secure old data.

Within the last ten years, *pp* elastic scattering has been extensively measured at LAMPF (650–800 MeV), Saturne II (800–2800 MeV), and SIN (440–590 MeV). The bulk of this recent data is concentrated above 440 MeV,

TABLE I. Beam and target configurations for data at 241, 314, 341, 366, 398, and 473 MeV. The symbol "Acc" stands for data taken with the accelerated beam and "Scatt" for data taken with the scattered beam. In both cases, the beam and target polarizations were frequently reversed. In this table, P stands for P_{n000}. For data taken with the CH_2 target, the magnetic field was switched off; therefore, the measured parameters do not contain any mixing of pure spin-dependent parameters ($\omega \equiv 0$).

Energy (MeV)	Beam orientation	Type of beam	Target	Center of angular range (deg)	Angular range (deg c.m.)	Measured parameters
241	$\pm X$	Acc	But. (+,−)	74	60–88	P, K_{n00n}, $D_{\omega 0s0}$, $M_{\omega 0s0}$
	$\pm Z$	Acc	But. (+,−)	74	60–88	P,K_{n00n}, $D_{\omega 0k0}$, $M_{\omega 0k0}$
	$\pm Y$	Acc	But. ϕ	74	60–88	P, D_{n0n0}
314	$\pm X$	Acc	But. (+,−)	74	60–88	P, K_{n00n}, $K_{\omega 0s0}$, $M_{\omega 0s0}$
	$\pm Z$	Acc	But. (+,−)	74	60–88	P, K_{n00n}, $D_{\omega 0k0}$, $M_{\omega 0k0}$
341	$\pm X$	Acc	CH_2	52	38–66	P, $D_{s'0s0}$
	$\pm X$	Acc	CH_2	84	70–98	P, $D_{s'0s0}$
	$\pm Z$	Acc	CH_2	52	38–66	P, $D_{s'0k0}$
	$\pm Z$	Acc	CH_2	84	70–98	P, $D_{s'0k0}$
	$\pm Y$	Acc	CH_2	52	38–66	P, D_{n0n0}
	$\pm Y$	Acc	CH_2	84	70–98	P, D_{n0n0}
366	$\pm Y$	Scatt	CH_2	52	38–66	P, D_{n0n0}
	$\pm Y$	Scatt	CH_2	84	70–98	P, D_{n0n0}
398	$\pm X$	Acc	But. (+,−)	52	38–66	P, K_{n00n}, $D_{\omega 0s0}$, $M_{\omega 0s0}$
	$\pm X$	Acc	But. (+,−)	84	70–98	P, K_{n00n}, $D_{\omega 0s0}$, $M_{\omega 0s0}$
	$\pm Z$	Acc	But. (+,−)	52	38–66	P, K_{n00n}, $D_{\omega 0k0}$, $M_{\omega 0k0}$
	$\pm Z$	Acc	But. (+,−)	84	70–98	P, K_{n00n}, $D_{\omega 0k0}$, $M_{\omega 0k0}$
473	$\pm Z$	Acc	CH_2	48	34–62	P, $D_{s'0k0}$

TABLE II. Results for the *pp* elastic-scattering parameters at 241 MeV. Quoted errors are purely statistical. The beam energies quoted correspond to the reaction energies at the center of the polarized target. The estimated uncertainty is about ±3 MeV. Uncertainties in the detectors and beam position lead to an uncertainty on the c.m. bin center value of ±0.25°.

$\theta_{c.m.}$ (deg)	P_{n000}	D_{n0n0}	K_{n00n}
60	0.324±0.023	0.416±0.085	0.405±0.045
64	0.242±0.014	0.558±0.054	0.442±0.028
68	0.210±0.013	0.425±0.049	0.463±0.025
72	0.156±0.013	0.524±0.050	0.472±0.025
76	0.120±0.014	0.429±0.053	0.469±0.026
80	0.071±0.014	0.557±0.055	0.483±0.028
84	0.034±0.015	0.598±0.059	0.494±0.030
88	−0.023±0.019	0.393±0.073	0.504±0.036

$\theta_{c.m.}$ (deg)	$D_{\omega 0s0}$	$D_{\omega 0k0}$	$M_{\omega 0sn}$	$M_{\omega 0kn}$	ω (deg)
60	0.198±0.044	0.081±0.050	0.379±0.081	−0.138±0.093	11.5
64	0.224±0.027	0.068±0.027	0.205±0.050	0.103±0.059	11.6
68	0.297±0.025	0.036±0.029	0.089±0.045	0.119±0.054	11.9
72	0.343±0.025	0.116±0.029	0.078±0.045	0.156±0.055	12.1
76	0.366±0.026	0.030±0.030	0.105±0.047	0.056±0.056	12.4
80	0.434±0.027	0.096±0.032	0.035±0.050	0.108±0.060	12.7
84	0.443±0.030	0.118±0.035	0.047±0.054	0.167±0.065	13.0
88	0.461±0.036	0.104±0.042	−0.010±0.065	0.069±0.078	13.4

so any interpretation of the data (phase-shift analyses, potential models) below this energy, relies on rather dated (1965) measurements and on a rather restrictive choice of spin-dependent parameters (mainly A_{00nn} and A_{00kk}).[9] For instance, the violent low-energy dependence of A_{00nn} at 90° c.m. (Ref. 1) and the fact that A_{00nn} (90° c.m.) equals one at 140 MeV, is based on a single experiment with few data points and with 5% absolute error.

We have, therefore, performed measurements at six energies: 241, 314, 341, 366, 398, and 473 MeV. For technical reasons, it was not possible to degrade the beam energy any lower.

II. EXPERIMENTAL SETUP

A complete description of the experimental setup can be found in Refs. 2 and 10.

TABLE III. Same as Table II but at 314 MeV.

$\theta_{c.m.}$ (deg)	P_{n000}	K_{n00n}
60	0.317±0.011	0.527±0.021
64	0.286±0.010	0.526±0.018
68	0.242±0.009	0.534±0.017
72	0.186±0.009	0.525±0.017
76	0.163±0.009	0.549±0.017
80	0.095±0.009	0.546±0.017
84	0.045±0.010	0.546±0.018
88	0.013±0.013	0.549±0.023

$\theta_{c.m.}$ (deg)	$D_{\omega 0s0}$	$D_{\omega 0k0}$	$M_{\omega 0sn}$	$M_{\omega 0kn}$	ω (deg)
60	0.391±0.022	0.122±0.022	0.209±0.040	0.034±0.039	10.4
64	0.421±0.019	0.125±0.018	0.239±0.034	0.055±0.033	10.5
68	0.480±0.018	0.146±0.018	0.184±0.033	0.092±0.032	10.7
72	0.484±0.018	0.156±0.017	0.136±0.033	0.101±0.032	10.9
76	0.555±0.018	0.163±0.017	0.123±0.033	0.155±0.031	11.1
80	0.542±0.018	0.164±0.017	0.058±0.033	0.178±0.032	11.4
84	0.565±0.018	0.141±0.018	0.004±0.034	0.165±0.033	11.6
88	0.608±0.024	0.106±0.024	0.051±0.045	0.145±0.043	12.0

TABLE IV. Same as Table II but at 341 MeV.

$\theta_{c.m.}$ (deg)	P_{n000}	D_{n0n0}	$D_{s'0s0}$	$D_{s'0k0}$
38	0.411±0.038	0.405±0.077	0.072±0.097	−0.034±0.090
42	0.426±0.017	0.516±0.036	0.177±0.041	−0.016±0.042
46	0.410±0.011	0.514±0.024	0.181±0.026	−0.013±0.027
50	0.388±0.010	0.505±0.021	0.234±0.022	0.053±0.023
54	0.355±0.009	0.539±0.020	0.295±0.021	0.126±0.022
58	0.315±0.009	0.546±0.019	0.357±0.020	0.158±0.021
62	0.263±0.008	0.597±0.019	0.414±0.019	0.195±0.020
66	0.225±0.010	0.555±0.022	0.403±0.023	0.258±0.024
70	0.237±0.014	0.627±0.031	0.465±0.031	0.286±0.033
74	0.163±0.011	0.579±0.024	0.399±0.024	0.289±0.026
78	0.112±0.010	0.607±0.024	0.496±0.023	0.319±0.025
82	0.075±0.010	0.592±0.023	0.543±0.024	0.268±0.025
86	0.038±0.011	0.655±0.024	0.486±0.024	0.248±0.026
90	−0.014±0.011	0.586±0.025	0.540±0.025	0.183±0.027
94	−0.059±0.012	0.646±0.028	0.533±0.027	0.281±0.030
98	−0.096±0.020	0.651±0.045	0.491±0.045	0.214±0.049

Two types of polarized beams were used for these experiments: (1) a "scattered" beam which was obtained by scattering the main SIN unpolarized beam at 8° from an 8-mm-thick Be target (polarization $P_b = 0.4165 \pm 0.0043$) and (2) an "accelerated" beam in which polarized protons were produced directly by the atomic source and then accelerated to 580 MeV ($P_b \simeq 0.8$ typically).

The polarized proton beam was scattered from a polarized target (PPT), cylindrical in shape, 2 cm in height and 2 cm in diameter. The target sample, composed of frozen butanol droplets immersed in liquid ^{3}He at ~ 0.5 K was placed in a 25-kG vertical magnetic field. Target polarizations P_t varied between 40% and 60%. A dummy target of the same size, consisting of carbon grains, was suspended below the butanol target, and could be raised in the beam for background measurements.

A few data were also taken with a CH_2 target. These data allowed us to measure the polarization parameters (P_{n000}, D_{n0n0}) independently of the target polarization.

Scattered and recoil particles were detected by two X-Y telescopes, each consisting of three multiwire proportional chambers and a scintillation counter. The spin of the scattered proton was analyzed in a carbon polarimeter mounted directly behind the scattered proton telescope. Each telescope was mounted on a movable platform, which could be rotated about the target axis so as to allow measurement of different angular ranges. A summary of all different beam and/or target conditions under which data were collected is given in Table I. The axes $(\hat{\mathbf{x}}, \hat{\mathbf{y}}, \hat{\mathbf{z}})$ refer to the fixed laboratory frame of the apparatus, where $\hat{\mathbf{z}}$ corresponds to the direction of the incident beam and $\hat{\mathbf{y}}$ to the vertical downward direction.

The beam energies quoted correspond to the reaction energies at the center of the polarized target. The estimated uncertainty is about ±3 MeV.

III. ANALYSIS

Throughout this paper we will use the scattering matrix and formalism of Ref. 11. A very detailed description of the choice of observables and analysis has already been published, along with the data between 440 and 579 MeV (Refs. 2–4). One should refer to these papers for more complete information. Here we will just mention relevant points for the understanding of this paper.

The measured observables are listed in Table I. The four-index notation X_{abcd} refers to the scattered (a), recoil (b), beam (c), and target (d) spin orientations. Each index (a, b, c, or d) can take either values k, n, s, or 0 according based on a Fourier analysis.[12]

The measured observables are listed in Table I. The four-index notation X_{abcd} refers to the scattered (a), recoil (b), beam (c), and target (d) spin orientations. Each index (a, b, c, or d) can take either values k, n, s, or 0 according to the particle polarization orientation in its attached laboratory frame. The direction $\hat{\mathbf{k}}$ is defined as being along the particle trajectory, $\hat{\mathbf{n}}$ along the normal to the scattering plane, and $\hat{\mathbf{s}}$ orthogonal to the other two axes

TABLE V. Same as Table II but at 366 MeV.

$\theta_{c.m.}$ (deg)	P_{n000}	D_{n0n0}
38	0.426±0.022	0.497±0.054
42	0.445±0.012	0.529±0.030
46	0.420±0.011	0.500±0.027
50	0.379±0.010	0.512±0.025
54	0.328±0.010	0.569±0.024
58	0.308±0.009	0.524±0.025
62	0.274±0.009	0.592±0.022
66	0.221±0.010	0.567±0.024
70	0.202±0.018	0.578±0.042
74	0.155±0.013	0.587±0.031
78	0.135±0.012	0.567±0.030
82	0.081±0.012	0.562±0.030
86	0.037±0.013	0.550±0.030
90	−0.018±0.013	0.646±0.031
94	−0.063±0.014	0.548±0.035
98	−0.129±0.021	0.508±0.050

$(\hat{\mathbf{n}}\times\hat{\mathbf{k}})$. The 0 index stands for an unpolarized state. Where confusion can occur, indices for the scattered particle will be indicated with primes, i.e., s' and k'.

The index ω, present in some parameters of Table I, has been introduced to indicate that we have measured, at the carbon scatterer, a mixture of s' and k' components of the true hydrogen scattering: this is an effect of the magnetic field of the PPT. It has been shown[2] that the magnetic field effect can be treated as a rotation around the veritcal axis $\hat{\mathbf{n}}$ by an angle ω. For this reason the horizontal transverse polarization of the scattered particle measured at the carbon analyzing target contains a mixture of the s' and k' components. The measured observables are, therefore, given by

$$X_{\omega}\ldots = \cos\omega\, X_{s'}\ldots - \sin\omega\, X_{k'}\ldots \ , \tag{1}$$

where X is any polarization parameter.

IV. RESULTS AND CONCLUSIONS

The experimental results are given in Tables II–VII, along with their statistical errors, for each energy. The

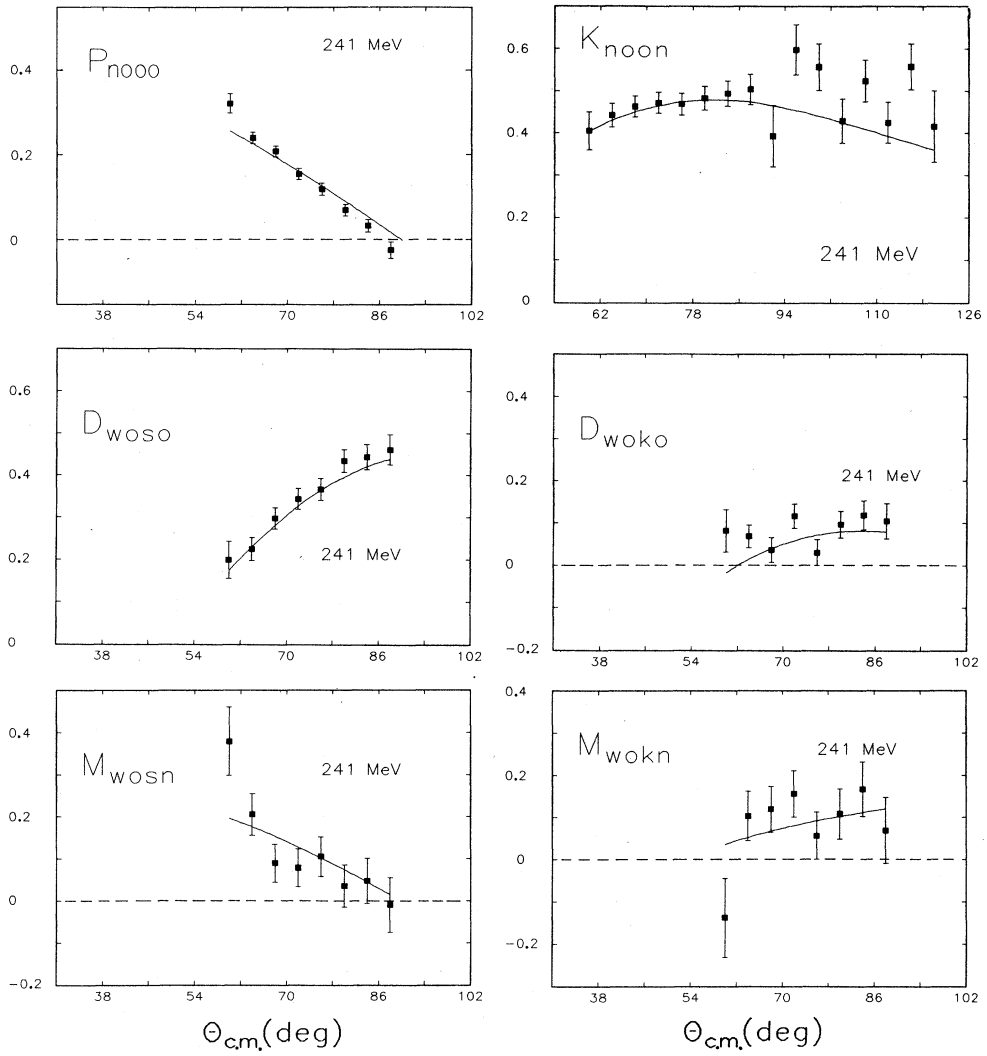

FIG. 1. Results for the *pp* elastic spin parameters at 241 MeV plotted as a function of the c.m. scattering angle shown as a solid square ■. K_{n00n} and D_{n0n0} have been plotted together using their symmetry relation around 90° c.m. [see Eq. (2)]. The solid line is the fit obtained from the Saclay-Geneva PSA (Ref. 13). Other available data where they exist within ±14 MeV around the nominal beam kinetic energy are indicated in the figures with the following symbols: ◆, Ref. 14; ▽, Ref. 15; △, Ref. 16; ○, Ref. 17; and ×, Ref. 9 for older data.

TABLE VI. Same as Table II but at 398 MeV.

$\theta_{c.m.}$ (deg)	P_{n000}	K_{n00n}
38	0.480±0.020	0.296±0.039
42	0.496±0.013	0.445±0.025
46	0.454±0.011	0.422±0.022
50	0.403±0.011	0.489±0.020
54	0.361±0.010	0.501±0.019
58	0.320±0.009	0.518±0.018
62	0.281±0.009	0.535±0.018
66	0.249±0.009	0.569±0.018
70	0.218±0.011	0.585±0.022
74	0.166±0.010	0.583±0.019
78	0.123±0.010	0.575±0.018
82	0.104±0.009	0.608±0.018
86	0.015±0.009	0.620±0.018
90	0.004±0.009	0.602±0.018
94	−0.054±0.010	0.599±0.019
98	−0.102±0.012	0.594±0.023

$\theta_{c.m.}$ (deg)	$D_{\omega 0s0}$	$D_{\omega 0k0}$	$M_{\omega 0sn}$	$M_{\omega 0kn}$	ω (deg)
38	0.246±0.037	−0.089±0.039	0.393±0.072	−0.210±0.075	9.0
42	0.284±0.025	−0.041±0.024	0.432±0.048	−0.195±0.047	9.1
46	0.280±0.021	0.039±0.021	0.316±0.041	−0.156±0.041	9.2
50	0.377±0.020	0.121±0.020	0.353±0.038	−0.051±0.038	9.3
54	0.411±0.019	0.150±0.019	0.309±0.036	−0.102±0.036	9.4
58	0.494±0.018	0.235±0.018	0.272±0.034	0.038±0.034	9.5
62	0.525±0.017	0.254±0.017	0.307±0.033	0.118±0.033	9.6
66	0.536±0.018	0.255±0.018	0.208±0.035	0.125±0.034	9.7
70	0.559±0.020	0.238±0.023	0.211±0.039	0.220±0.045	9.9
74	0.554±0.017	0.248±0.020	0.108±0.033	0.159±0.039	10.1
78	0.613±0.017	0.240±0.020	0.066±0.033	0.247±0.038	10.3
82	0.593±0.017	0.202±0.020	−0.074±0.033	0.326±0.038	10.5
86	0.630±0.017	0.187±0.020	0.019±0.032	0.316±0.038	10.7
90	0.642±0.017	0.173±0.020	−0.026±0.032	0.298±0.038	11.0
94	0.612±0.017	0.154±0.020	0.013±0.033	0.288±0.039	11.3
98	0.642±0.021	0.091±0.025	−0.068±0.041	0.319±0.049	11.7

mixing angle ω for each $\theta_{c.m.}$ bin is also quoted. Figures 1–6 show the results as a function of the c.m. scattering angle. In Figs. 1 and 6, one has made use of the symmetry relation

$$D_{n0n0}(\theta_{c.m.}) = K_{n00n}(\pi - \theta_{c.m.}) \quad (2)$$

for plotting our measured data in order to present the results in one single plot. All other available data, within ±14 MeV of the quoted kinetic energy, are also shown on the figures. One sees immediately that data for the polarization parameter P_{n000} have been abundantly measured, but much less so far the two-spin parameters. Data for the three-spin parameters are nonexistent. The explanation of the different symbols are given in the caption of Fig. 1. In general, a good agreement with previously measured data is found. For the 314-MeV results, where previous data for the two-spin parameters existed in the surrounding energy region, we have shown in Fig. 6, in addition to the parameters P_{n000} and D_{n0n0}, the pure spin parameters $R\,(D_{s'0s0})$ and $A\,(D_{s'0k0})$ in order to ease the comparison with existing data. To extract these quantities, we have made use of Eq. (1) in which the values for the $R'(D_{k'0s0})$ and $A'(D_{k'0k0})$ parameters were taken

TABLE VII. Same as Table II but at 473 MeV.

$\theta_{c.m.}$ (deg)	P_{n000}	$D_{s'0k0}$
34	0.510±0.060	0.006±0.078
38	0.505±0.030	−0.002±0.039
42	0.480±0.024	0.089±0.031
46	0.438±0.022	0.121±0.029
50	0.397±0.021	0.272±0.028
54	0.408±0.020	0.371±0.026
58	0.310±0.019	0.370±0.025
62	0.287±0.022	0.367±0.028

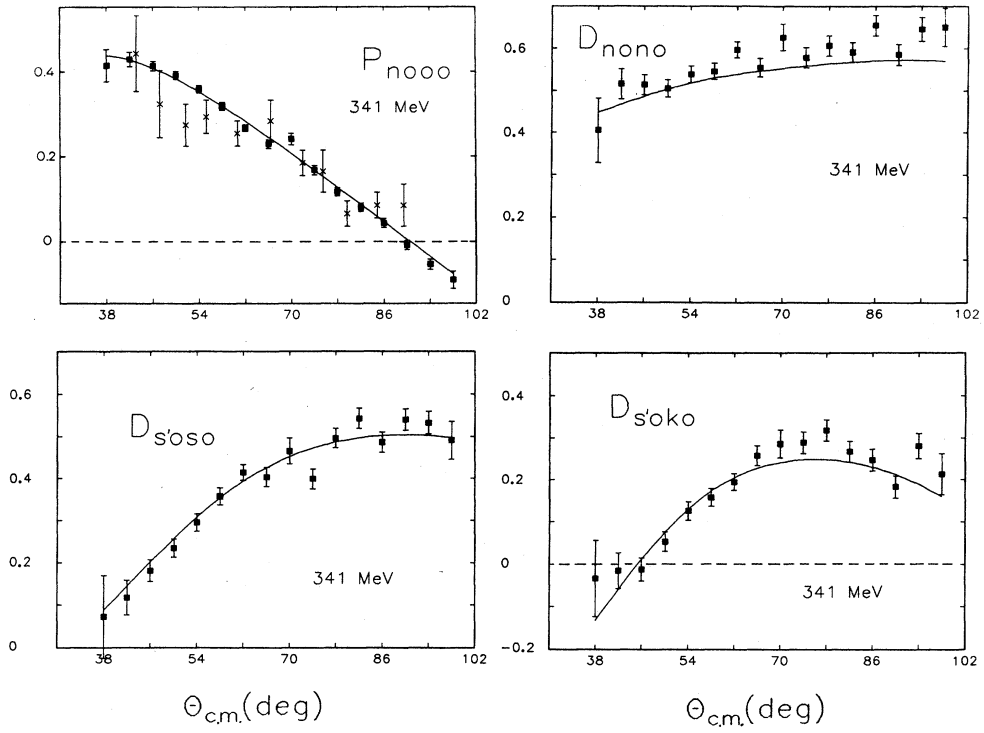

FIG. 2. Same as Fig. 1 but at 341 MeV. See caption of Fig. 1 for explanation of the symbols.

from the phase-shift-analysis (PSA) predictions.[13] This allows one to observe a smooth continuation towards small angles as measured at SIN (Ref. 14).

The solid line is the fit obtained from the Saclay-Geneva PSA (Ref. 13). As this PSA is performed in energy intervals, we have used the so-called "260-MeV" interval (134–460 MeV) containing almost all the data points. The overall χ^2 value for these 296 data points is 477. No problem was found in the fit: This is not surprising as the PSA predictions obtained from a previous solution (not containing these data) is close. However, these data have better constrained the *pp* phases, reducing the error bars by 10%.

A careful study of the possible systematic errors has been performed (as developed in Ref. 6). A test of the internal consistency of the data measured with different

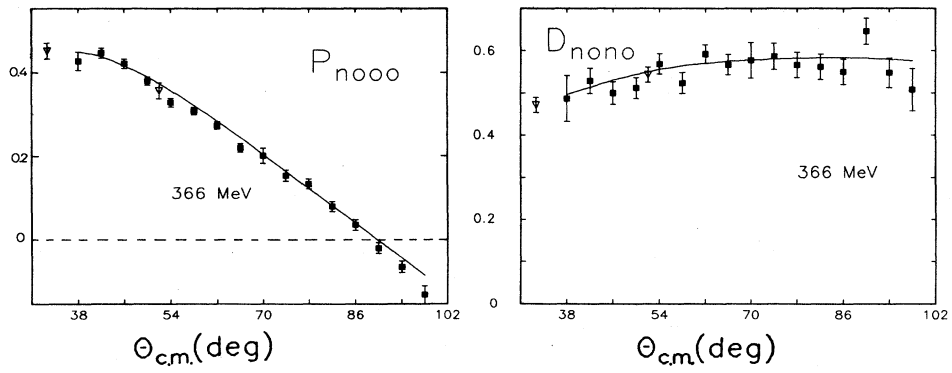

FIG. 3. Same as Fig. 1 but at 366 MeV. See caption of Fig. 1 for explanation of the symbols.

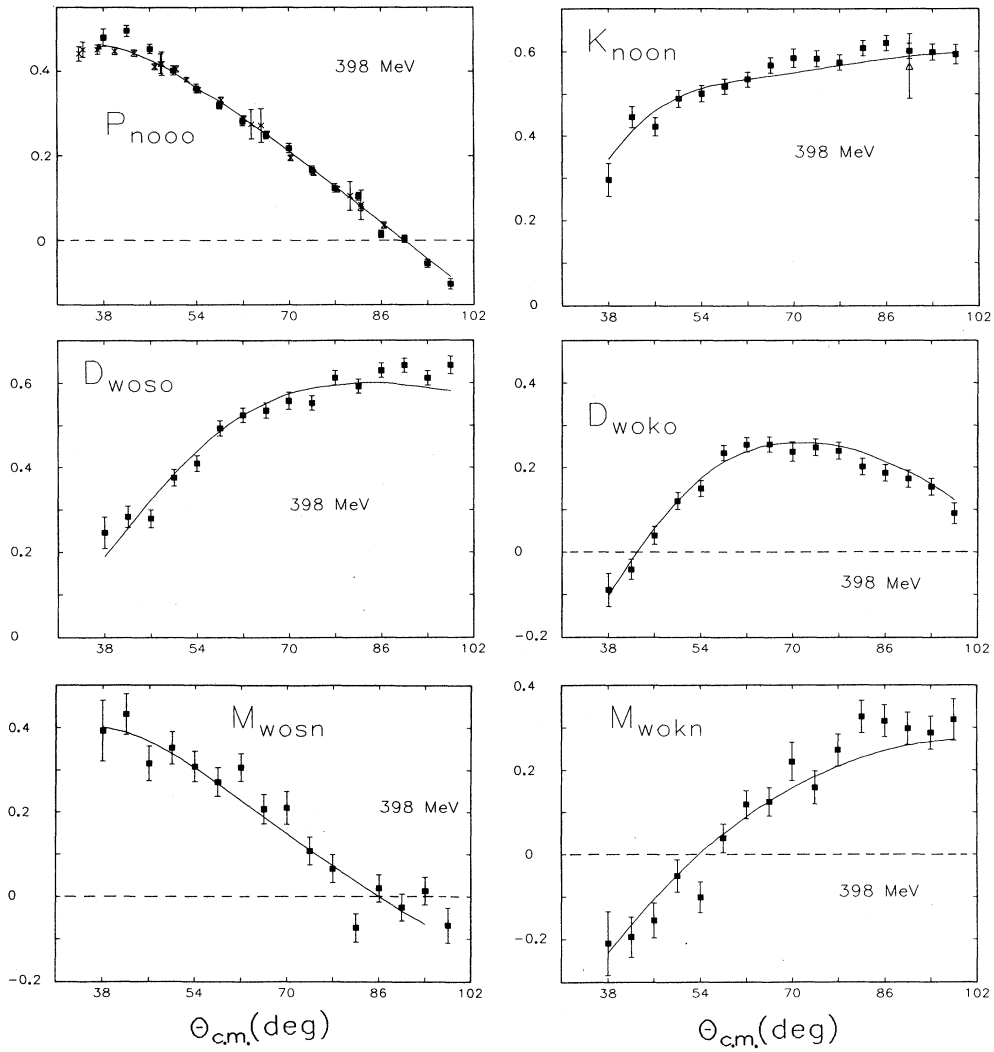

FIG. 4. Same as Fig. 1 but at 398 MeV. See caption of Fig. 1 for explanation of the symbols.

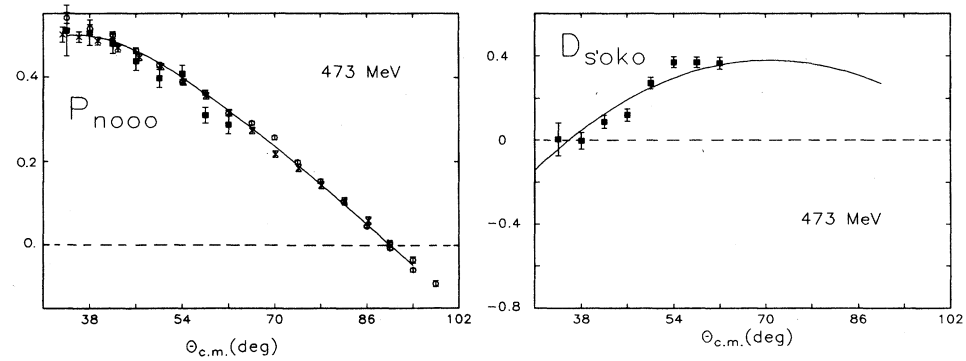

FIG. 5. Same as Fig. 1 but at 473 MeV. See caption of Fig. 1 for explanation of the symbols.

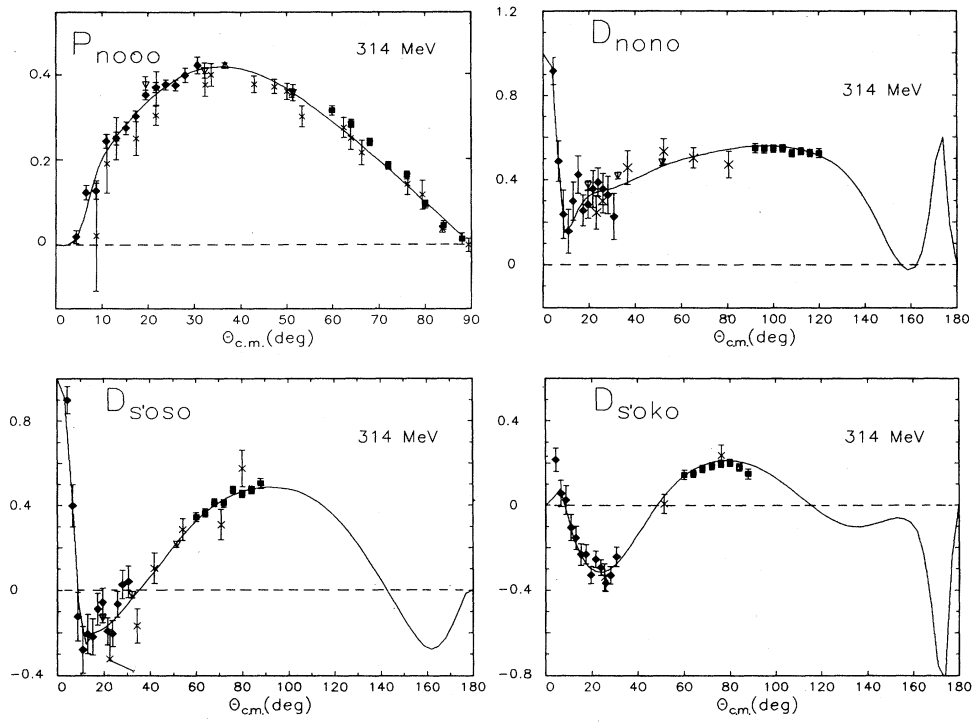

FIG. 6. P_{n000}, D_{n0n0}, $D_{s'0s0}$, and $D_{s'0k0}$ spin parameters at 314 MeV. See caption of Fig. 1 for explanation of the symbols. D_{n0n0} was obtained from K_{n00n} using their symmetry relation around 90° c.m. [see Eq. (2)]. The two last pure spin parameters were calculated from the measured mixed parameters $D_{\omega 0s0}$ and $D_{\omega 0k0}$ as explained in the text [see Eq. (1)].

beam/target orientations is given by the overall χ^2 obtained in the fitting procedure used to extract the parameters at each angle. A typical value of $\chi^2/\nu \sim 1.1$ was observed. Relative systematic errors due to uncertainties on the beam and target polarizations and carbon analyzing power are summarized as follows: 3% on P, 7% on K, 4% on D, 8% on M. For data taken with the "scattered beam," the beam polarization is better known, so that the two last values become 2% on D and 6% on M.

In conclusion, these data have confirmed and secured previous old and limited measurements. These measurements complete our experimental program at SIN, and confirm the PSA solutions found previously.

ACKNOWLEDGMENTS

We would like to thank the Paul Scherrer Institute for its valuable technical assistance and express our special gratitude to its director, Professor J. P. Blaser. We would like to thank the technical staff of the University of Geneva. This work was supported by the Swiss National Science Foundation.

*Present address: Department of Physics, Iowa University, Iowa City, IA 52242.

†Present address: LeCroy, route du Nant-d'Avril 101, 1217 Meyrin, Switzerland.

‡Present address: OFAC, rue Pedro-Meylan 7, 1208 Geneva, Switzerland.

§Present address: Ecole d'Ingénieurs du Canton de Neuchâtel-ETS, 2400 Le Locle, Switzerland.

[1]D. Besset, Q.H. Do, B. Favier, R. Hausammann, C. Lechanoine-Leluc, W. R. Leo, D. Rapin, D. W. Werren, Ch. Weddigen, J. M. Cameron, S. Jaccard, and S. Mango, Nucl. Phys. **A345**, 435 (1980).

[2]E. Aprile, R. Hausammann, E. Heer, R. Hess, C. Lechanoine-Leluc, W. R. Leo, S. Morenzoni, Y. Onel, D. Rapin, and S. Mango, Phys. Rev. D **27**, 2600 (1983).

[3]E. Aprile, R. Hausammann, E. Heer, R. Hess, C. Lechanoine-Leluc, W. R. Leo, S. Morenzoni, Y. Onel, D. Rapin, and S. Mango, Phys. Rev. D **28**, 21 (1983).

[4]E. Aprile, R. Hausammann, E. Heer, R. Hess, C. Lechanoine-Leluc, W. R. Leo, S. Morenzoni, Y. Onel, D. Rapin, P. Y. Rascher, S. Jaccard, J. A. Konter, and S. Mango, Phys. Rev. D **34**, 2566 (1986).

[5]E. Aprile, C. Eisenegger, R. Hausammann, E. Heer, R. Hess, C. Lechanoine-Leluc, W. R. Leo, S. Morenzoni, Y. Onel, and D. Rapin, Phys. Rev. Lett. **46**, 1047 (1981).

[6]R. Hausammann, Ph.D. thesis, University of Geneva, 1982, No. 2038.

[7]C. Lechanoine-Leluc, in *Proceedings of the VII International Symposium on High Energy Spin Physics,* Protvino, USSR, 1986 (Institute of High Energy Physics, Serpukhov, 1987), pp. 199–208.

[8]R. Hausammann, E. Heer, R. Hess, C. Lechanoine-Leluc, Y.

Onel, and D. Rapin Phys. Rev. D **40**, 22 (1989).
[9]J. Bystricky and F. Lehar, in Nucleon-Scattering Data, edited by H. Behrens and G. Ebel (Physics Data Nos. 11-1, 11-2, and 11-3) (Fachinformationszentrum, Karlsruhe, 1978 and 1981).
[10]D. Besset, Q. H. Do, B. Favier, L. G. Greeniaus, E. Heer, R. Hess, C. Lechanoine-Leluc, D. Rapin, D. W. Werren, M. Daum, S. Mango, E. Steiner, G. Vecsey, and Ch. Weddigen, Nucl. Instrum. Methods **184**, 365 (1981)
[11]J. Bystricky, F. Lehar, and P. Winternitz, J. Phys. (Paris) **39**, 1 (1978).
[12]D. Besset, B. Favier, L. G. Greeniaus, R. Hess, C. Lechanoine, D. Rapin, and D. W. Werren, Nucl. Instrum. Methods **166**, 515 (1979).
[13]J. Bystricky, C. Lechanoine-Leluc, and F. Lehar, J. Phys. (Paris) **48**, 199 (1987).
[14]D. Besset, Q. H. Do, B. Favier, L. G. Greeniaus, R. Hess, C. Lechanoine, D. Rapin, D. W. Werren, and Ch. Weddingen, Phys. Rev. D **21**, 580 (1980).
[15]D. Axen, F. Felawka, S. Jaccard, J. Vavza, G. Ludgate, N. Stewart, C. Amsler, R. Brown, D. Bugg, J. Edgington, C. Oram, K. Shakarchi, and A. Clough, Lett. Nuovo Cimento **20**, 151 (1977).
[16]C. L. Hollas, D. J. Cremans, R. D. Ransome, P. J. Riley, B. E. Bonner, M. W. McNaughton, and S. Wood, Phys. Lett. **143B**, 343 (1984).
[17]E. Aprile, R. Hausammann, E. Heer, R. Hess, C. Lechanoine-Leluc, W. R. Leo, S. Morenzoni, Y. Onel, D. Rapin, P. Y. Rascher, S. Jaccard, J. A. Konter, and S. Mango, Phys. Rev. D **34**, 2566 (1986).